

JafaLK

by Jafa Lk

Submission date: 15-Aug-2021 08:10AM (UTC+0700)

Submission ID: 1631419648

File name: Photogram.pdf (816.22K)

Word count: 2844

Character count: 14832

PAPER • OPEN ACCESS

Photogrammetric stereo image rectification

6

To cite this article: M E Tjahjadi and F Handoko 2021 *J. Phys.: Conf. Ser.* **1869** 012066

View the [article online](#) for updates and enhancements.



ECS **240th ECS Meeting**
Oct 10-14, 2021, Orlando, Florida

**Register early and save
up to 20% on registration costs**

Early registration deadline Sep 13

REGISTER NOW



Photogrammetric stereo image rectification

M E Tjahjadi^{1,*} and F Handoko²

¹ Department of Geodesy, National Institute of Technology (ITN) Malang, Jl. Bendungan Sigura-gura 2 Malang 65145

² Department of Industrial Engineering, National Institute of Technology (ITN) Malang, Jl. Bendungan Sigura-gura 2 Malang 65145

*edwin@lecturer.itn.ac.id

Abstract. Today, off-the-shelf digital cameras are hand on tools for conducting visual inspections in surveying and mapping related activities or in structural inspection of industrial objects. Dense point clouds of the inspected object surface are of typical data required and their accuracies are also become more demanding. Deriving these data are off particular interest of this paper instead we work on overlapping images for generating those ones. An imaging geometry of stereo images is exploited further to reveal some drawbacks of the normalized stereo imaging configurations. We utilize a photogrammetric collinearity condition to model physical reality of the imaging process. A sequence of coordinate axes rotations on both images is rearranged as well as preserving normalized images resolutions to be equal to the source ones. Also based upon the prescribed resolutions, an efficient indirect resample is performed to interpolate grey values of the warped images. To ascertain reliability of the mathematically developed method, C++ programming codes were written and implemented in the solution. It reveals that a nuisance such as y-parallax is completely eliminated. Therefore, by using our method, the normalized images can be used in the dense point clouds production in a high quality and efficiency.

1. Introduction

In our ongoing research project conducting aerial and terrestrial photography, there is a need to inspect three dimensional object through stereoscopic viewing [1] for a variety of photogrammetric image processing tasks [2,3]. Stereoscopic viewing is established by rectifying two overlapping images of the same rigid scene undergo projective transformations [4]. Then, a resampling is performed to produce an image pair that has the corresponding epipolar lines coincide and be parallel to x-axis of images. Nonetheless, barely any captured images are ready for viewing geometry due to cumbersome image processing tasks. An alternative method is sought to be more intuitive and simple to make images are geometrically ready for stereoscopic viewing.

The epipolar rectification enables disparities between two images is only in the x-axis direction or lie on the same rows. Many algorithms are relied on a homographic or a fundamental matrix [5] to estimate the correspondence point and minimize perspective distortion. A more accurate algorithm using a so called three step image rectification to minimize camera rotations had been invented [6]. Both algorithms use homographic matrices on one or two images to rectify the image, but an undesirable distortion still occurs due to an exclusion of camera lens distortion model.



A method called normalized images [7] was invented to resample epipolar images with respect to the world or object space reference system. The images are in epipolar geometry with respect to the object space. Following this idea, this paper discusses a modified version of their work by adding additional parameters of systematic errors such as lens distortion. Digital consumer grade cameras are widely known to suffer instabilities in their internal lenses and electronics imaging system [8]. Recently, quite similar works have been reported [9–11], but they use known Ground Control Point coordinates instead of an arbitrary coordinate frame. The next section explains some background knowledge followed by a detailed elaboration of how to obtain an aligned and rectified stereo images with an arbitrary object space coordinate system.

2. Methods

A relationship between the original stereo pair and its normalized pair is established by connecting the perspective centre of the left image and its rectified image (C_1) together with the right image and its rectified one (C_2) respectively (Figure 1). It is assumed that the interior parameters (i.e., x_p, y_p, c), exterior parameters (X_{C1}, Y_{C1}, Z_{C1}) for the left image and (X_{C2}, Y_{C2}, Z_{C2}) for the right image, as well as camera calibration parameters (i.e., $K_1, K_2, K_3, P_1, P_2, a_1, a_2$) are known. The epipolar geometry of a stereo pair is the geometry of the intersection of the image planes with the planes containing the baseline B . It intersects each original image plane at the left epipole (e_1) and the right epipole (e_2). The baseline vector of B_x, B_y , and B_z components intersects each original image plane at the left epipolar line and the right epipolar line respectively. Any point $A(X, Y, Z)$ in the object space appears both on actual images at a'_1 and a'_2 as well as on rectified ones at a_1 and a_2 as depicted in Figure 1.

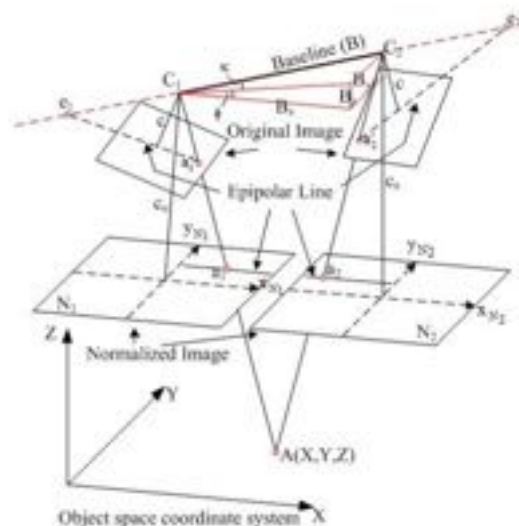


Figure 1. A relationship between original and normalized stereo pair.

Aforementioned parameters above can be computed using an approximate but fast method [12], or by a rigorous methods such space resection [13] or relative orientation [14]. The collinearity condition [13] stated that the object space point A, and its corresponding image as well as normalized one are formed a straight line to the perspective centre C_1 and C_2 of the original images. The equation to relate a point from the original image to the object space and from the normalized image to the object space and their rotational elements are as follows [7]:

$$[x - x_p \quad y - y_p \quad -c]^T = R_b R^T [x_N \quad y_N \quad -c]^T \quad (1)$$

$$[B_x \ B_y \ B_z]^T = [X_{c2} - X_{c1} \ Y_{c2} - Y_{c1} \ Z_{c2} - Z_{c1}]^T \quad (2)$$

$$\Omega = (\omega_1 + \omega_2) \cdot 2^{-1}; \quad \phi = \tan^{-1}(B_x B_x^{-1}); \quad K = \tan^{-1}(B_y [B_x^2 + B_z^2]^{-0.5}) \quad (3)$$

R_b is the rotation matrices normalized images where R is a rotation matrix of original image [13]. The baseline component vectors are required to rotate and align original images to the normalized ones. The process can be viewed as a two steps of rotation. The first steps, the viewing directions of the original images are rotated to a perpendicular with the normal direction of the X-Y axes of the object space plane. This yields a true parallel with Z axis of object space system. The second steps, it makes x-y axes of once rotated image align with the X-Y axes of the object space system. The result is a normalized stereo pairs of N_1 and N_2 which their x axes are parallel with the X axis and their y axes are parallel with the Y axis. A combination of these three elementary rotations into the baseline rotation R_b yields:

$$R_b = R_K R_\phi R_\Omega = \begin{bmatrix} \cos K & \sin K & 0 & \cos \phi & 0 & -\sin \phi & 1 & 0 & 0 \\ -\sin K & \cos K & 0 & 0 & 1 & 0 & 0 & \cos \Omega & \sin \Omega \\ 0 & 0 & 1 & \sin \phi & 0 & \cos \phi & 0 & -\sin \Omega & \cos \Omega \end{bmatrix} \quad (4)$$

If those two rotations are combined, it would transform the original image into the normalized position. The transformation (4) must be done twice for a stereo pair with using each of its extrinsic parameter rotation where for the left image $R_{N1} = R_b R_1^T$ and $R_{N2} = R_b R_2^T$ for the right one. If distortion free stereo images are used the value of the resulting y parallax will be zero or negligible. However due to utilization of consumer grades, off-the-shelves cameras, the exhibit lens distortion should be eliminated during the process of stereo rectification. Using equation (1), the relationship between the original and normalized image can be expressed by the modified collinearity equation as [15]:

$$x - x_p - \Delta x = -c(r_{11}x_N + r_{21}y_N - r_{31}c)(r_{13}x_N + r_{23}y_N - r_{33}c)^{-1} \quad (5a)$$

$$y - y_p - \Delta y = -c(r_{21}x_N + r_{22}y_N - r_{32}c)(r_{13}x_N + r_{23}y_N - r_{33}c)^{-1} \quad (5b)$$

$$\Delta x = \bar{x}r^2K_1 + \bar{x}r^4K_2 + \bar{x}r^6K_3 + P_1(r^2 + 2\bar{x}^2) + 2P_2\bar{x}\bar{y} + a_1\bar{x} + a_2\bar{y} \quad (5c)$$

$$\Delta y = \bar{y}r^2K_1 + \bar{y}r^4K_2 + \bar{y}r^6K_3 + P_2(r^2 + 2\bar{y}^2) + 2P_1\bar{x}\bar{y} + 2P_3\bar{x}\bar{y} \quad (5d)$$

$$\bar{x} = x - x_p; \quad \bar{y} = y - y_p; \quad r = (\bar{x}^2 + \bar{y}^2)^{-0.5} \quad (5e)$$

Both x , y and x_N , y_N are image coordinates in metric unit (i.e. mm). $\Delta x, \Delta y$ are systematic lens distortion errors from optical and electronic components of the camera. Neglecting these terms will cause a projected collinear ray on the image will deviate from its true position. Also, r_{11}, \dots, r_{33} are the element of R_{N1} , or R_{N2} . In this paper it is assumed that the focal lengths for all type of images are equal. This equation is applied for each image, and it is usually easier to project the tessellation of the normalized image back to the original image to determine the grey level.

The procedure to rectify according to the epipolar line [7] starts from the transformation T_1 (Figure 2). T_1 enables pixel addresses of the original digital image to be transformed to a camera system and vice versa. T_2 is the projective transformation between the original and rectified images. Equation 1 is used to transform coordinates from an original image to its normalized counterpart or to transform coordinates from the normalized image to the original image by using an inverse process of it. T_2 defines the origin and size of the normalized digital image. First, the four corners of the original digital image ((0, 0), (max column, 0), (max column, max row), and (0, max row)) are transformed to the normalized image coordinates through T_1 and T_2 . The origin of the normalized digital image is calculated by determining the maximum y-coordinate, which determines row = 0. The minimum x coordinate defines

column = 0. For the size of the normalized digital image, the maximum coordinate differences, dx_{max} and dy_{max} , in x and y directions are computed.

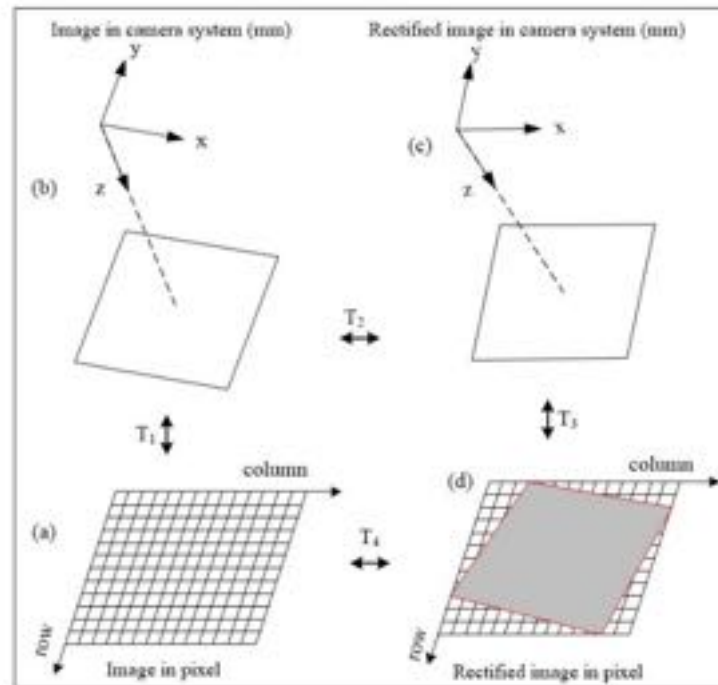


Figure 2. A relationship between the original and normalized stereo pair.

A change from the normalized image coordinates to normalized pixel coordinates is performed by using the relations $dx_{max} = \text{resolution in } x' \text{ direction}$, and $dy_{max} = \text{resolution in } y' \text{ direction}$. Two options are available to determine the size of the normalized digital image. The first keeps the original resolution. The created normalized digital image will have a different pixel size from the original one. The second retains the original pixel size, but it has a different number of pixels (or different resolutions). T_4 involves epipolar rectification between the original digital image and the normalized one. The transformation is accomplished using indirect differential rectification [16] and each pixel tessellation is calculated through T_3 , T_2 , and T_1 as illustrated in Figure 2.

3. Results and discussion

Data for the demonstration are two unrectified stereo images (Figure 3) with known interior and exterior orientation parameters. The algorithm above is implemented in C++, developed algorithms are applicable for grey value images only, however they can be extended to input colour images.

After determining the origin and size of the normalized stereo, tessellation grids of these images are ready to be filled in by grey values from the originals which are done through T_4 transformation. Bilinear interpolation is chosen to resample grey values. A pair of the normalized images is created: the preserving resolution pair (Figure 4 left-column) and the preserving pixel size pair (Figure 4 right-column).

There is a possibility of the loss of information on normalized images due to the choice of interpolation method as well as resolutions and pixel sizes. The effect of the loss of information is noticeable. Blurring effects in all patches are caused by employing the bilinear interpolation method.

However, the use of option preserving resolution (Figure 4 left-column) may result in corrupted edge information. It was revealed that the corrupted edges can affect a process of stereoscope viewing. Hence, this option is not recommended. The normalized images from option preserving pixel size (Figure 4 right-column) also have drawbacks. The computational time is much greater than that of the first option. Moreover, the resulting normalized image file size generated using this option is bigger than that from using the other one. However, this option would result the most accurate epipolar line location which can produce a zero y parallax.

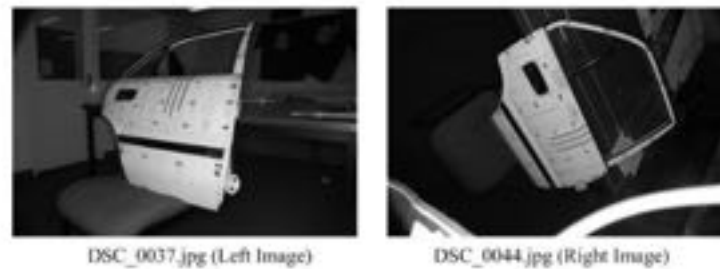


Figure 3. Input stereo pair.

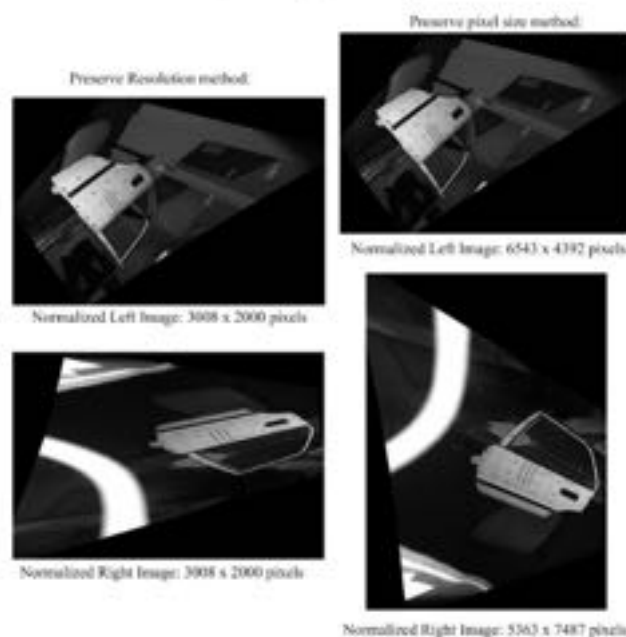


Figure 4. Two methods of normalizing stereo pair.

This method results distortion-less stereo images since it incorporates camera distortion parameters while performing image rectification process. Another improvement of this method is that two different resolutions of stereo image can be produced due to the Ω rotation. A choice of preserving pixel size would result a zero y-parallax and it is the most accurate epipolar line location. Furthermore, this method can align epipolar lines with geodetic reference frame provided that stereo images' exterior orientation parameters are supplied with GPS coordinates.

4. Conclusion

Epipolar rectification of a stereo pair with respect to the object space and by adding systematic errors of lens distortion as well as electronic imaging defect terms is important in the digital image processing. This method can align epipolar lines parallel to the axes of the any reference frame system. This method successful and operational to eliminate the y-parallax and to make the resulted epipolar line truly aligned with the Y axis of the reference system. When the image is rotated, the net area becomes larger. Maintaining the image resolution causes the pixel size larger, but maintaining a constant pixel size requires a higher resolution image. Furthermore, a developed C++ program for precise stereo image rectification is successfully implemented.

11. Acknowledgments

This work was funded by Ministry of Research, Technology and Higher Education of the Republic of Indonesia.

References

- [1] Li S, Ma L and Ng Ngan K 2013 Anaglyph image generation by matching color appearance attributes *Signal Process. Image Commun.* **28** 597–607
- [2] Tjahjadi M E, Handoko F and Sai S S 2017 Novel image mosaicking of UAV's imagery using collinearity condition *Int. J. Electr. Comput. Eng.* **7** 1188–96
- [3] Kedzierski M and Delis P 2016 Fast Orientation of Video Images of Buildings Acquired from a UAV without Stabilization *Sensors* **16** 1–16
- [4] Herráez J, Denia J L, Navarro P, Rodríguez J and Martín M T 2013 Epipolar image rectification through geometric algorithms with unknown parameters *J. Electron. Imaging* **22** 1–11
- [5] Hartley R I 1999 Theory and Practice of Projective Rectification *Int. J. Comput. Vis.* **35** 115–27
- [6] Monasse P, Morel J-M and Tang Z 2010 Three-step image rectification *BMVC 2010-British Machine Vision Conference* (BMVA Press) pp 89.1–89.10
- [7] Cho W and Schenk T 1992 Resampling Digital Imagery to Epipolar Geometry ed L W Fritz and J R Lucas *Int. Arch. Photogramm. Remote Sens.* **29** 404–8
- [8] Wackrow R, Chandler J H and Bryan P 2007 Geometric consistency and stability of consumer-grade digital cameras for accurate spatial measurement *Photogramm. Rec.* **22** 121–134
- [9] Liu J, Guo B, Jiang W, Gong W and Xiao X 2016 Epipolar rectification with minimum perspective distortion for oblique images *Sensors (Switzerland)* **16** 1–17
- [10] Jannati M, Valadan Zoj M J and Mokhtarzade M 2018 A novel approach for epipolar resampling of cross-track linear pushbroom imagery using orbital parameters model *ISPRS J. Photogramm. Remote Sens.* **137** 1–14
- [11] Liansheng S, Jiulong Z and Duwu C 2009 Image rectification using affine epipolar geometric constraint *J. Softw.* **4** 27
- [12] Tjahjadi M E 2016 A fast and stable orientation solution of three cameras-based UAV imageries *ARPN J. Eng. Appl. Sci.* **11** 3449–55
- [13] Tjahjadi M E and Handoko F 2017 Single frame resection of compact digital cameras for UAV imagery *International Conference on Electrical Engineering, Computer Science and Informatics (EECSI)* vol 4, ed M A Riyadi, M Facta, D Setiawan and H Rahmawan (Yogyakarta: IEEE Computer Society Press) pp 409–13
- [14] Tjahjadi M E and Agustina F D 2019 Fast and stable direct relative orientation of UAV-based stereo pair *Int. J. Adv. Intell. Informatics* **5** 24–39
- [15] Förstner W, Wrobel B, Paderes F, Fraser C S, Dolloff J, Mikhail E M, Rujikietgumjorn W and McGlone J C 2013 Analytical Photogrammetric Operations *Manual of Photogrammetry: 6th Edition* ed J C McGlone (Bethesda, Maryland: American Society for Photogrammetry and Remote Sensing) pp 785–955
- [16] Novak K 1992 Rectification of Digital Imagery *Photogramm. Eng. Remote Sens.* **58** 339–44

ORIGINALITY REPORT

16%

SIMILARITY INDEX

11%

INTERNET SOURCES

16%

PUBLICATIONS

8%

STUDENT PAPERS

PRIMARY SOURCES

- 1 C Tho, Y Heryadi, L Lukas, A Wibowo. "Code-mixed sentiment analysis of Indonesian language and Javanese language using Lexicon based approach", Journal of Physics: Conference Series, 2021 3%
Publication

- 2 José Herráez, José Luis Denia, Pablo Navarro, Jaime Rodríguez, M. Teresa Martín. "Epipolar image rectification through geometric algorithms with unknown parameters", Journal of Electronic Imaging, 2013 2%
Publication

- 3 repository.tudelft.nl 2%
Internet Source

- 4 Thomas Luhmann, Stuart Robson, Stephen Kyle, Jan Boehm. "Close-Range Photogrammetry and 3D Imaging", Walter de Gruyter GmbH, 2020 2%
Publication

- 5 A Maspupah, A Rahmani, J L Min. "Comparative study of regression testing 1%

tools feature on unit testing", Journal of
Physics: Conference Series, 2021

Publication

6	repository.syekhnurjati.ac.id Internet Source	1 %
7	psgsv.gsi.go.jp Internet Source	1 %
8	E D Daryono, I N G Wardana, C Cahyani, N Hamidi. "Biodiesel production process without glycerol by-product with base catalyst: effect of reaction time and type of catalyst on kinetic energy and solubility", IOP Conference Series: Materials Science and Engineering, 2021 Publication	1 %
9	M Delina, T S Oktafiandariato, R Fahdiran. "The volcanic ash dispersion simulation of Soputan with PUFF Lagrangian method", Journal of Physics: Conference Series, 2021 Publication	1 %
10	ijain.org Internet Source	1 %
11	www.mdpi.com Internet Source	1 %
12	eprints.itn.ac.id Internet Source	1 %

13

Martinus Edwin Tjahjadi, Fourry Handoko.
"Single frame resection of compact digital
cameras for UAV imagery", 2017 4th
International Conference on Electrical
Engineering, Computer Science and
Informatics (EECSI), 2017

Publication

1 %

Exclude quotes Off

Exclude matches < 1%

Exclude bibliography On